A Fermi-Ulam model with regular and stochastic perturbations

Diogo Ricardo da Costa[1,2], Carl P. Dettmann[3] and Edson D. Leonel[1]

[1]Universidade Estadual de Ponta Grossa (UEPG); [2]Departamento de Física, UNESP - Univ Estadual Paulista, Rio Claro - SP - Brazil; [3]School of Mathematics, University of Bristol, United Kingdom.

ABSTRACT

Some statistical properties related to the diffusion in energy for an ensemble of classical particles in a bouncing ball model are studied. The particles are confined to bounce between two rigid walls. One of them is fixed while the other oscillates. The dynamics is described by a two dimensional nonlinear map for the velocity of the particle and time at the instant of the collision. Two different types of change of momentum are considered: (i) periodic due to a sine function and; (ii) stochastic. For elastic collisions case (i) leads to finite diffusion in energy while (ii) produces unlimited diffusion. On the other hand, inelastic collisions yield either (i) and (ii) to have limited diffusion. Scaling arguments are used to investigate some properties of the transport coefficient in the chaotic low energy region. Scaling exponents are also obtained for both conservative and dissipative case for cases (i) and (ii). We show that the parameter space has complicated structures either in Lyapunov as well as period coordinates. When stochasticity is introduced in the dynamics, we observed the destruction of the parameter space structures. This is a reviw of a paper accepted for publication in 2014 [1].

THE MODEL, THE MAP AND NUMERICAL RESULTS

The model we consider is a simplified version of the Fermi-Ulam model[2]. It consists of a classical particle - or an ensemble of non-interacting particles - confined to bounce between two rigid walls. Because of the simplification both walls are assumed to be fixed. However when the particle collides with one of them, say the one in the left, it suffers an exchange of energy and momentum due to the collision as if the wall were moving. The other wall is introduced as a returning mechanism for the particle to collide again with the wall responsible for the exchange of energy. Considering dimensionless variables (see [3]), the mapping that describes the dynamics of the particle is written as

$$T:\begin{cases}\phi_{n+1}=[\phi_n+\frac{2}{v_n}+2\pi\delta Z]\mod(2\pi)\\ v_{n+1}=|\alpha v_n-(1+\alpha)\epsilon\sin(\phi_{n+1})|\end{cases},\qquad(1)$$

where $\alpha\in[0,1]$ denotes the restitution coefficient, $\epsilon\in[0,1]$ corresponds to amplitude of the maximum velocity of the *moving wall* and $\delta\in[0,1]$ corresponds to the strength of the stochastic perturbation. Let us discuss more on the stochastic perturbation. Indeed in a real experiment, the position of the moving wall is given by an external engine with limited power. Of course the stochastic perturbation could be interpreted as due to imperfections of the system. As for example the engine suffering influences of external noise, like electric fluctuations, therefore causing disturbs to the motion of the moving wall. Additionally, one may think the particle, which in an experiment could be a sphere, has also imperfections in the shape. Most likely such imperfections could lead the particle to rotate, transferring translational energy to rotational. All of these terms can be modelled by a stochastic perturbations. The term $Z\in[0,1)$ is a uniform random number obtained by using a generator RAN2 in Fortran code.

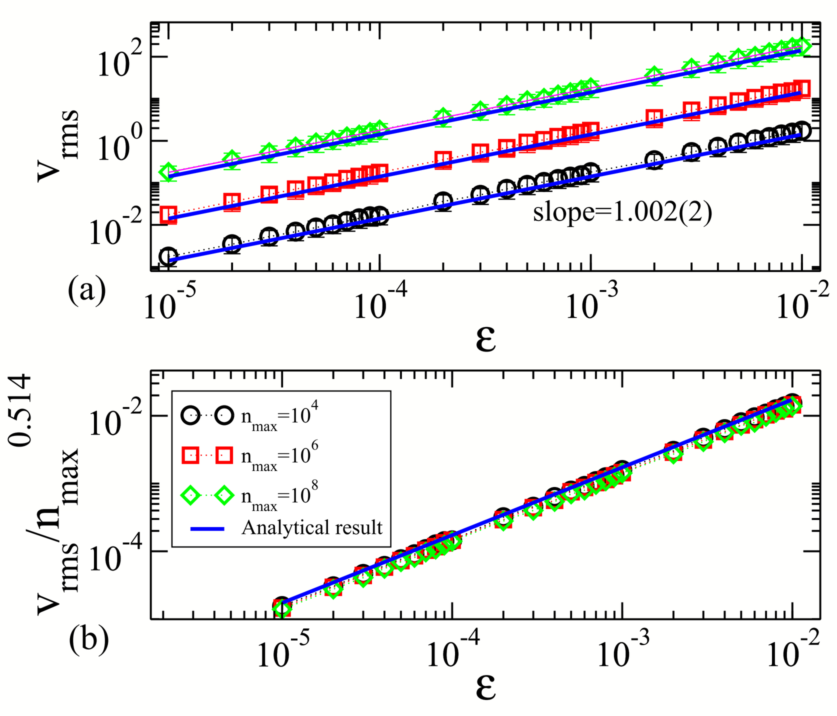

Fig. 1) Plot of: (a) v_{rms} as a function of ϵ for three different values of the maximum number of iterations n_{max} namely ($n_{max}=10^4$, $n_{max}=10^6$ and $n_{max}=10^8$). (b) Rescale of the vertical axis for the curves shown in (a) after the transformation $\bar{v}\rightarrow\bar{v}/n_{max}^{0.514}$. The analytical results are shown as blue straight lines.

Considering the second equation of the map (1), we can show after an ensemble average that

$$\overline{v_{n+1}^2}=\alpha^2\overline{v_n^2}+\frac{(1+\alpha)^2}{2}\epsilon^2,\qquad(2)$$

where $\overline{v^2}$ corresponds to the average of v^2. In the conservative case $\alpha=1$ the average (RMS) velocity grows with an exponent 1 with respect to ϵ and 1/2 with respect to n:

$$v_{rms}=\sqrt{\overline{v^2}}=\sqrt{v_0^2+2\epsilon^2 n}\ ,\qquad(3)$$

for large n, or small v_0 (see Fig. [1]).

In the paper analytical results for the root mean square velocity (v_{rms}) are calculated when $\alpha<1$. For $n\rightarrow\infty$ we find

$$v_{rms}=v_{sat}=\sqrt{(1+\alpha)/2}(1-\alpha)^{-1/2}\epsilon\ .\qquad(4)$$

Therefore, $\overline{v}_{sat}\propto\epsilon^{\alpha_1}(1-\alpha)^{\alpha_2}$ and we thus have $\alpha_1=1$ and $\alpha_2=-0.5$. Considering small values of v_0 in the Eq. (3) and equating to Eq. (4), we find the crossover n_x given by the followin equation

$$n_x=\left(\frac{1+\alpha}{4}\right)(1-\alpha)^{-1}\ .\qquad(5)$$

The crossover n_x scales as $(1-\alpha)^{-1}$ independent of ϵ. Therewith, $n_x\epsilon^2\propto\epsilon^{z_1}(1-\alpha)^{z_2}$ we thus have $z_1=2$ and $z_2=-1$.

The RMS velocity gives only a single measure of the distribution. We propose that the above exponents apply more generally, and test this by considering the deviation around of the average velocity defined as

$$\omega(n,\epsilon,\alpha)=\frac{1}{M}\sum_{k=1}^{M}\sqrt{\overline{v_k^2}(n,\epsilon,\alpha)-\overline{v_k}^2(n,\epsilon,\alpha)}.\qquad(6)$$

Here M denotes an ensemble of different initial conditions. Using ω we obtained the same values for z_1 and z_2.

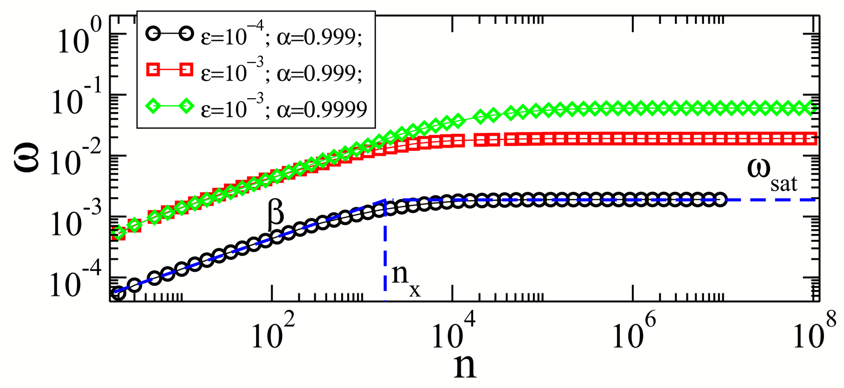

Fig. 2) Plot of ω vs n for three different values of ϵ and α. The slope of growth is $\beta\cong0.5$ obtained after a power law fit. The saturation and crossover are indicated in the figure.

Histograms and diffusion coefficient

In the paper[1] we study the histogram for the number of particles that reached certain height h. We end up with a decay of the histogram after reaching the peak at n_p described by $H\propto\exp[-Dn\pi^2/h^2]$. Here D is the diffusion coefficient. Indeed D can be written as $D=4h^2\mu/\pi^2$, where $\mu=(1-\alpha)^{z_2}$. We also show that

$$\overline{v_{n+1}^2}-\overline{v_n^2}=\left\langle\Delta^2\right\rangle=\overline{v_n^2}(\alpha^2-1)+\frac{(1+\alpha)^2}{2}\epsilon^2.$$

In the limit of $\alpha\cong1$ but still less than 1, the diffusion coefficient is then given by $D\cong\langle\Delta^2\rangle/2$. We conclude in the limit of $\alpha\cong1$ that $D/[(1+\alpha)^2\epsilon^2]\cong1/4$ for the initial velocity $v_0\rightarrow0$. The limit $D=1/4$ is shown in Figs. 5(b,c) as dashed lines.

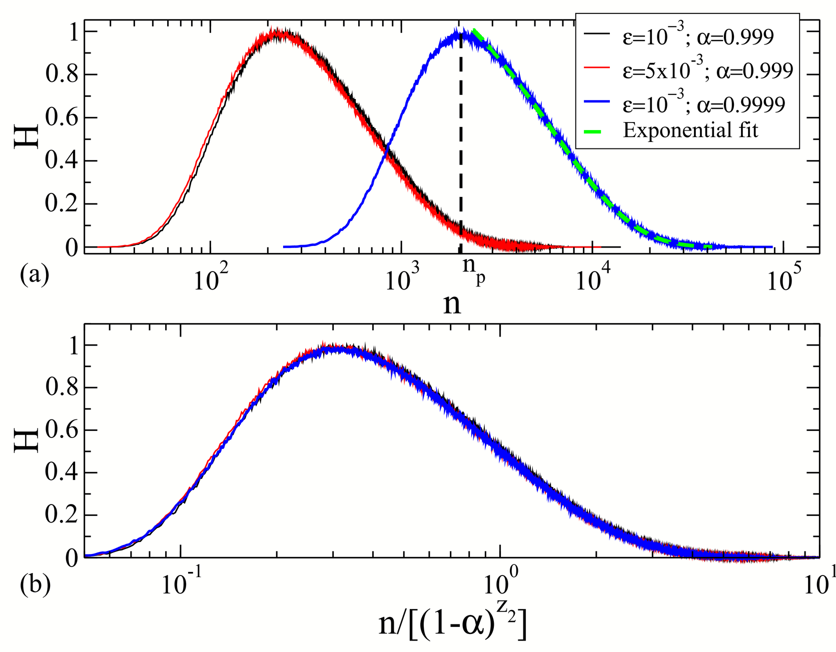

Fig. 3) Plot of: (a) histogram of frequency for the number of particles that have reached h as a function of the number of collisions n for different control parameters. (b) Overlap of (a) onto a single and universal plot after a rescaling of the horizontal axis.

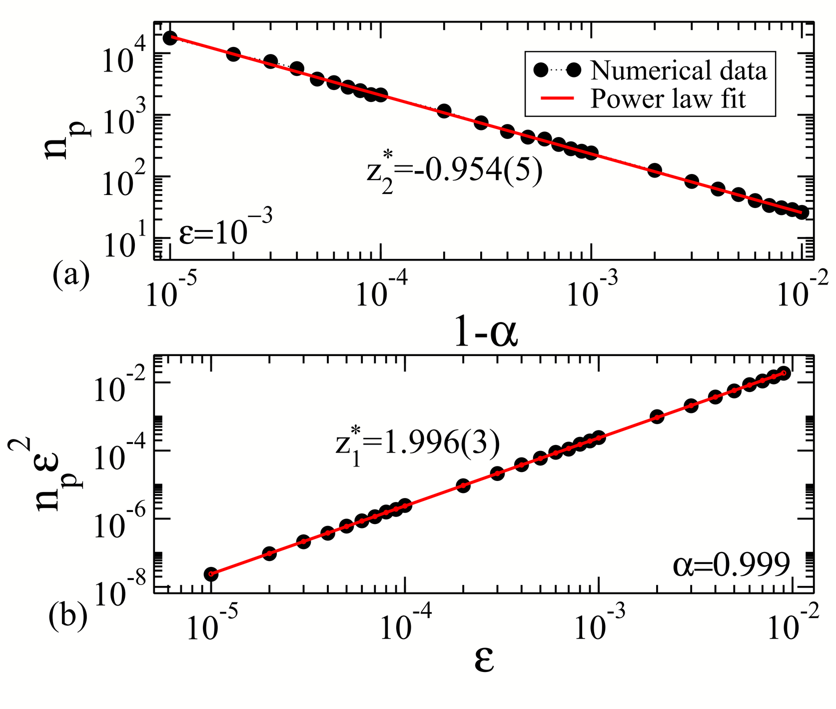

Fig. 4) Plot of: (a) n_p vs $(1-\alpha)$ for $\epsilon=10^{-3}$; (b) $n_p\epsilon^2$ vs ϵ using $\alpha=0.999$.

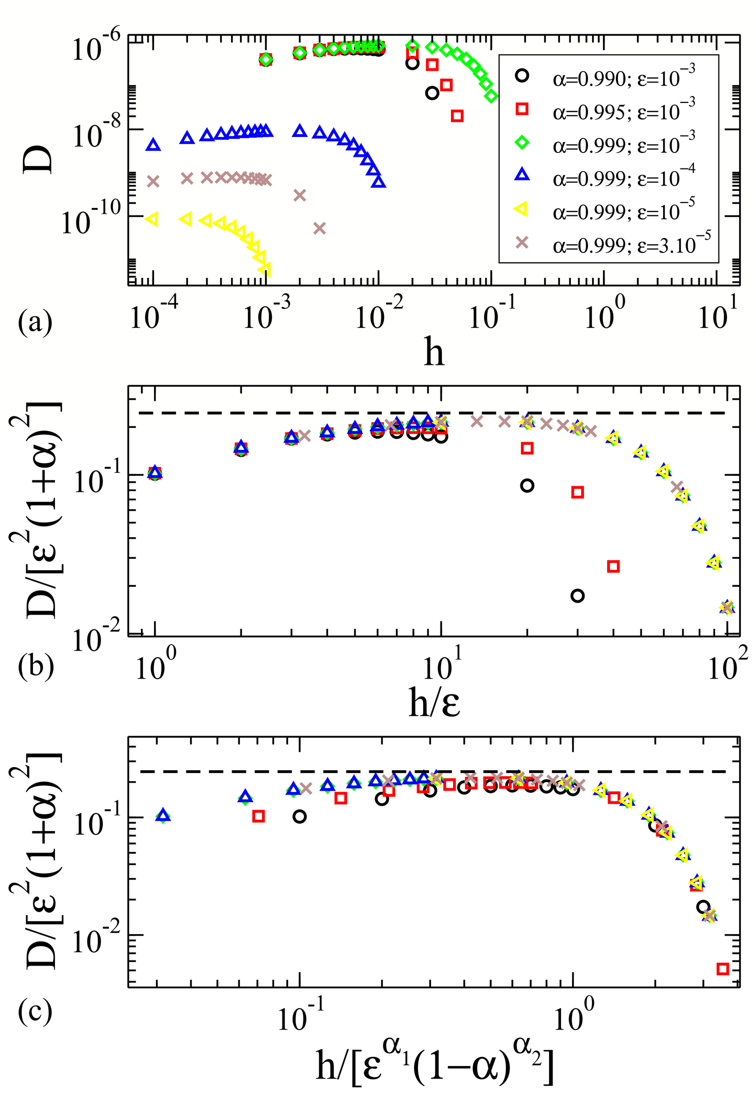

Fig. 5) Plot of: (a) D vs h for different values of α and ϵ; (b) overlap for all curves presented in (a) after a rescale of the axis for low values of h; (c) overlap of all curves presented in the item (a) after a proper rescale in the axis for high values of h.

Parameter space

The Lyapunov exponent can be obtained from

$$\lambda_j=\lim_{n\rightarrow\infty}\frac{1}{n}\ln|\Lambda_j{}^{(n)}|,\ j=1,2\qquad(7)$$

where $\Lambda_j{}^{(n)}$ are the eigenvalues of the matrix $\tilde{M}=\prod_i^n J_i(v_i,\phi_i)$ and J_i is the Jacobian matrix evaluated along the orbit (v_i,ϕ_i). If at least one of the λ_j is positive, then the system is said to have chaotic components. The colors in the Fig. 6(a,c,e,g,h) are Lyapunov exponents.

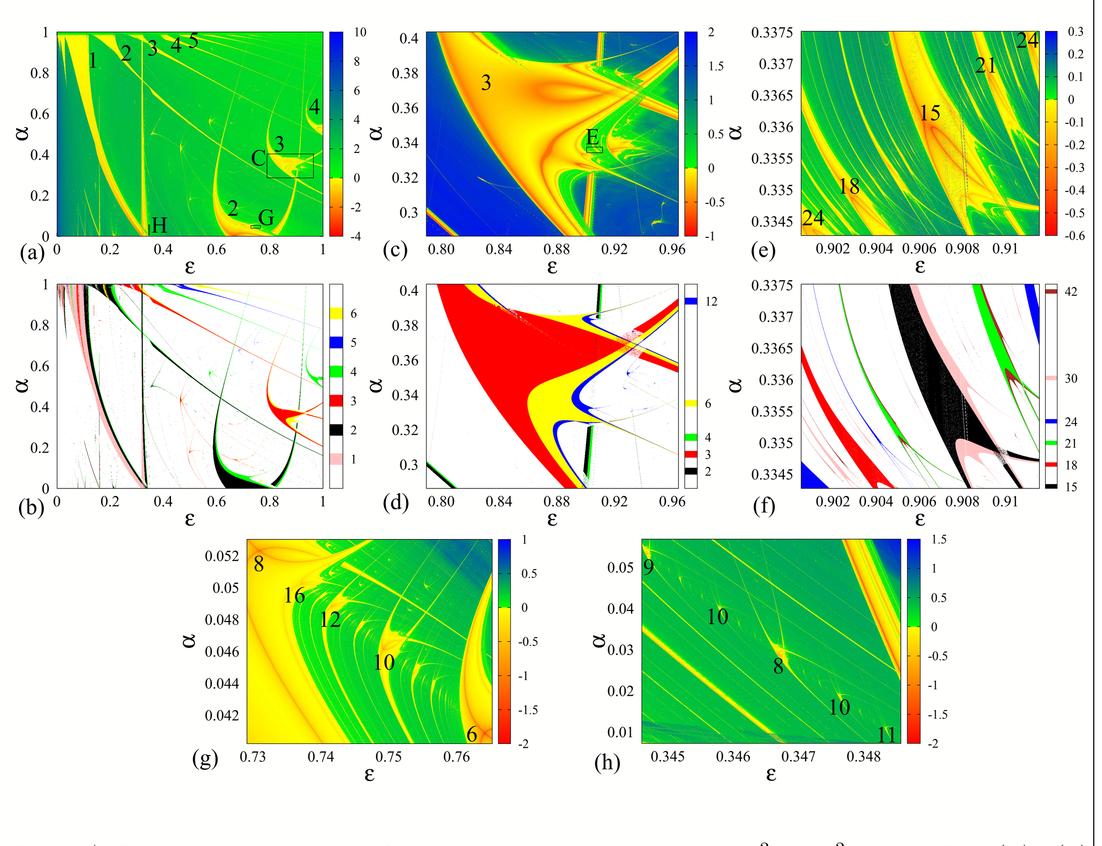

Fig. 6) Parameter space for $\delta=0$ considering a grid of $10^3\times10^3$ cells. For (a), (c), (e), (g) and (h) we present the maximum Lyapunov exponent, where the exponents were coded with a continuous colour scale ranging from red-yellow (negative exponents) to green-blue (positive exponents). For (b), (d) and (f) the colours represent the period. We have considered fixed initial conditions of $v_0=0.1$ and $\phi_0=6$.

Therefore the position of the periodic regions are given by: (i) for Fig. 6(e)

$$\alpha(\epsilon)=0.069(2)+0.295(3)\epsilon;\qquad(8)$$

(ii) for Fig. 6(g)

$$\alpha(\epsilon)=0.305(3)+0.346(4)\epsilon;\qquad(9)$$

and finally (iii) for Fig. 6(h)

$$\alpha(\epsilon)=4.09(5)+11.7(1)\epsilon.\qquad(10)$$

Considering that the organization of the periodic regions are described by the three equations above, we can use such relations to obtain the bifurcation diagrams for the variable velocity as a function of ϵ, as shown in Figs. 7(a,b,c) and using respectively Eqs. (8), (9) and (10).

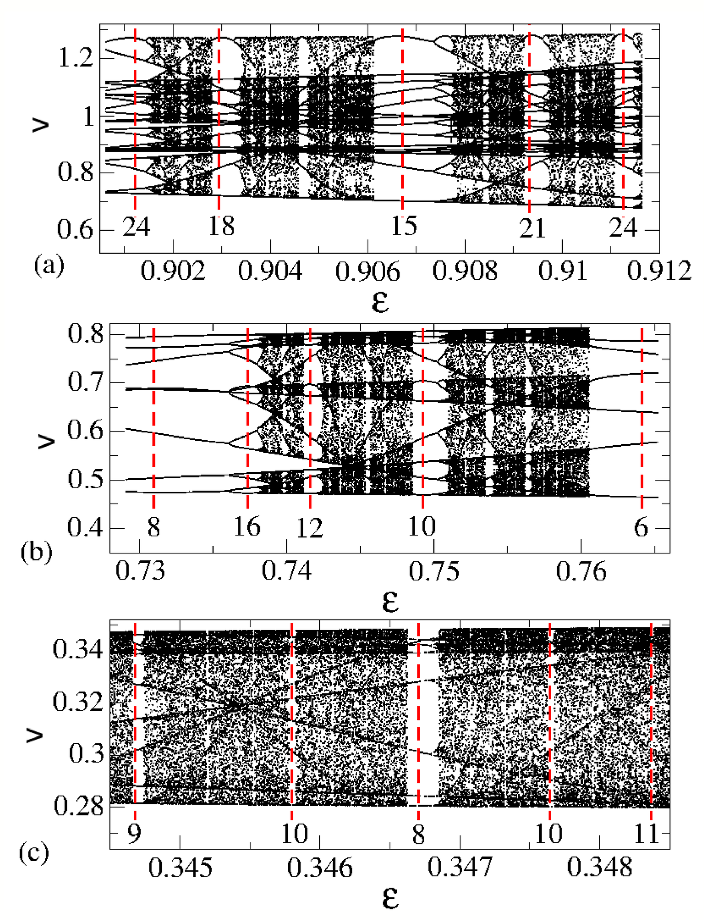

Fig. 7) Plot of a bifurcation diagram for the variable velocity as function of ϵ where α is given by the following expressions: (a) Eq. (8); (b) Eq. (9); (c) Eq. (10). We have considered fixed initial conditions of $v_0=0.1$ and $\phi_0=6$.

Fig. 8 shows the influence of δ in the parameter space.

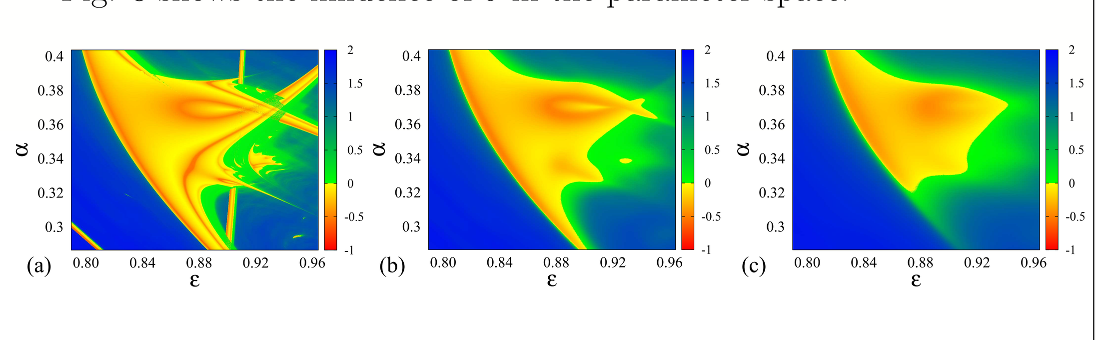

Fig. 8) Plot of the parameter space coloured by the Lyapunov exponent considering the same range of parameters as shown in Fig. 6(c). We considered different values of δ: (a) $\delta=0.00484$; (b) $\delta=0.00024$; (c) $\delta=0.01$.

REFERENCES

[1] Diogo R. da Costa, Carl P. Dettmann and Edson D. Leonel, Commun. Nonlinear Sci. Numer. Simulat. **20**, 871-881 (2015).
[2] A. J. Lichtenberg, M. A. Lieberman, Regular and Chaotic Dynamics. Appl. Math. Sci. 38, Springer Verlag, New York (1992).
[3] E. D Leonel, J. Phys. A: Math. Theor. **40**, F1077 (2007).